1st Latin-American Workshop on Structural Health Monitoring
LATAM-SHM 2023
December, 5-8 2023

DETECTING DEVIATING CELLS (DDC): AN OUTLIER FILTERING APPROACH FOR UNSUPERVISED DAMAGE DETECTION IN WIND TURBINES

Holger Cevallos-Valdiviezo[*], Moisés Benítez[*], Ricardo Prieto-Galarza[†,‡], Yolanda Vidal[†,△] and Christian Tutivén[†,◇]

[*] Facultad de Ciencias Naturales y Matemáticas, FCNM
Centro de Estudios e Investigaciones Estadísticas, CEIE
Escuela Superior Politécnica del Litoral, ESPOL
Campus Gustavo Galindo Km. 30.5 Vía Perimetral, P.O. Box 09-01-5863, Guayaquil, Ecuador
Phone number: +593 9 9103 5259,
e-mail: {holgceva, moibsori}@espol.edu.ec,
web page: https://www.espol.edu.ec

[†]Control, Data, and Artificial Intelligence, CoDAlab
Department of Mathematics, Escola d'Enginyeria de Barcelona Est, EEBE
Universitat Politècnica de Catalunya, UPC
Campus Diagonal-Besós (CDB) 08019, Barcelona, Spain
e-mail: {ricardo.prieto, yolanda.vidal}@upc.edu,
Web page: https://www.upc.edu/es

[‡]Universidad Ecotec
Km. 13.5 Samborondón, Samborondón, EC092302 Ecuador

[△]Institut de Matemàtiques de la UPC
BarcelonaTech, IMTech
Pau Gargallo 14, 08028 Barcelona, Spain

[◇]Mechatronics Engineering
Faculty of Mechanical Engineering and Production Science, FIMCP
Escuela Superior Politécnica del Litoral, ESPOL
Campus Gustavo Galindo Km. 30.5 Vía Perimetral, P.O. Box 09-01-5863, Guayaquil, Ecuador
Phone number: +593 9 9103 5259,
e-mail: cjtutive@espol.edu.ec,
web page: https://www.espol.edu.ec

Key words: wind turbine, structural health monitoring, damage detection, outlier filter

Abstract. Structural health monitoring plays a crucial role in ensuring the operational safety and performance of wind turbines. Detecting damage in a timely manner is essential to minimize downtime, mitigate risks, and ensure the long-term reliability of wind energy systems. In this study, a novel data-driven approach is proposed for early damage detection in wind turbines that utilizes the unsupervised outlier filter called "Detect Deviating Cells (DDC)". The approach uses triaxial accelerometer data collected from experimental wind turbines. By constructing a data matrix with columns representing triaxial accelerometer measurements and rows representing different time points, the outlier filter DDC is applied to identify wind

turbines with potential damage and determine the location and time at which the potential damage occurred through the detection of anomalous accelerometer measurements (cell-wise outlier detection). The experimental results demonstrate the promising potential of DDC for damage detection in wind turbines. In particular, DDC is an unsupervised technique that does not require prior labeling of wind turbine health status. This characteristic makes DDC suitable for SHM applications where the initial status of wind turbines is unknown and most of the data may originate from healthy turbines. Furthermore, DDC can be applied to recently acquired data, enabling the timely detection of damages without the need for costly and time-consuming inspections on site. This capability facilitates prompt repair actions and contributes to an effective, fast, and cost-efficient alternative for structural health monitoring. Wind turbine operators can use this approach to mitigate risks, optimize maintenance plans, and ensure the sustained reliability of wind energy systems.

1 Introduction

Offshore wind energy represents a significant and sustainable alternative, poised to play a pivotal role in mitigating carbon emissions in the quest for a greener future [1, 2]. The global shift towards renewable energy sources, exemplified by offshore wind power, is based on a deep commitment to environmental stewardship and an urgent response to the imperatives of climate change [3]. This transition is rooted in the recognition that offshore wind, in stark contrast to conventional fossil fuel-based electricity generation, exerts a much gentler ecological footprint, thus protecting the delicate balance of our ecosystems [4, 5]. Consequently, investments in wind turbines (WTs) have witnessed an unprecedented surge, boosted by ongoing technological advances that have enabled the installation of larger turbines in deeper waters, thus amplifying energy capacity [6]. However, this remarkable progress has not been without its challenges. The growing magnitude of WT size and capacity has ushered in a new era of apprehension, centered on the performance and safety of these towering structures. The passage of time has witnessed instances of structural damage and component faults, culminating in catastrophic accidents that have cast shadows on the reliability of this technology.

Structural health monitoring (SHM) is essential to ensure the safety of structures, especially offshore WTs. International standards, such as ISO guidelines, and national codes define precise methodologies for monitoring, sensor placement, data-driven health assessment, maintenance planning, and prediction of structural life [7]. SHM detects structural issues by analyzing responses to external stimuli [8].

Ensuring the safety and longevity of a WTs jacket structure is of paramount importance [9]. Traditional visual inspection methods serve as a common practice to identify surface-level issues, such as cracks, corrosion, and deformation, within the jacket structure. However, when it comes to detecting internal or difficult-to-reach damage, relying solely on visual inspection may prove inadequate. Vibration-based SHM, exemplified by [10], offers real-time monitoring, providing early warnings of potential damage, reducing costs, and preventing disasters. Also, with their established track record in damage identification for offshore platforms, hold promise for potential adaptation to WT jacket structures.

Recent research has explored diverse SHM techniques for offshore platforms and maritime structures. Kim et al. [11] employed cosine similarity, but faced computational challenges

with large data sets and similar damage patterns. Ye et al. [12] used finite element modeling, but struggled with computational costs due to complex offshore jacket structures. Zonzini [13] applied edge computing but faced resource constraints. Finally, Feijo et al. [14] show an unsupervised damage detection based on an autoencoder neural network, achieving very good results but with the high computational cost of training and performing inferences in a deep neural network. This work addresses the aforementioned limitations by using a computational low-cost outlier filter and only requiring 60 seconds of vibration data from the healthy structure and only 5 seconds of unknown structural state to identify when the jacket structure has a fault.

The article follows a structured format as indicated in the following. Section 2 presents the experimental setup. Section 3 indicates the damage scenario and the data acquisition process. Section 4 shows the damage detection methodology to follow, covering topics such as the construction of the composite matrix, normalization, and the deviation cell approach to detect damage. Section 5 gives a summary of the experimental results obtained. Finally, Section 6 presents the conclusions.

2 Experimental Setup

In this study, a scaled replica of an offshore jacket-type WT is used, boasting a height of 2.7 [m] and comprising three primary segments. The initial segment, designated as the nacelle, constitutes the apex of the WT, which encompasses a bar of dimensions 1 [m] in length and 0.6 [m] in width. At its left extremity, an inertial shaker of model Data Physics GW-IV47 is affixed, which is stimulated by a variety of excitation signals emanating from a function generator (GW INSTEK AF-2005) (see Figure 1 (left)). This generator provides various white noise amplitudes (factors of 0.5, 1, 2, and 3) to simulate the wind speeds encountered in different operational regions of the WT.

The subsequent segment is the tower, segmented into three portions interconnected by flanges. The tower extends to a length of 1.67 [m] with a diameter of 0.239 [m]. The final segment is the jacket, situated at the base, and is constructed from 32 S275JR steel bars, DC01 LFR steel plates, bolts, and nuts, the latter being tightened to a torque of 12 Nm. The jacket structure is organized into four levels, where level 1 is the one located deepest in the sea (in a real turbine) and level 4 is the one closest to the sea surface, as illustrated in Figure 1 (right).

To examine the dynamic behavior of the structure based on vibration measurement, eight triaxial accelerometers (PCB R Piezotronic, model 356A17) are deployed, and dispersed throughout the WT structure, as depicted in Figure 1. Given the triaxial nature of the sensors, a total of 24 vibration signals are procured. For the acquisition and processing of the signals measured by each accelerometer, six input modules of model NI 9234 by National Instruments are utilized, housed within a chassis (cDAQ model). For an in-depth exposition of the experimental setup, refer to [15].

This work endeavors to formulate a strategy adept at detecting crack damage in two different locations of the jacket support (levels 1 and 4) and only with a value of 3 for the shaker white noise amplitude (simulating only one region of operation). Figure 2 delineates a bar with a crack, where $\mathbf{L}$ denotes the length of the bar, $\mathbf{X} = \mathrm{L}/3$ signifies the distance of the crack from the left end of the bar, and $\mathbf{d}$ represents the size of the fissure (5 mm).

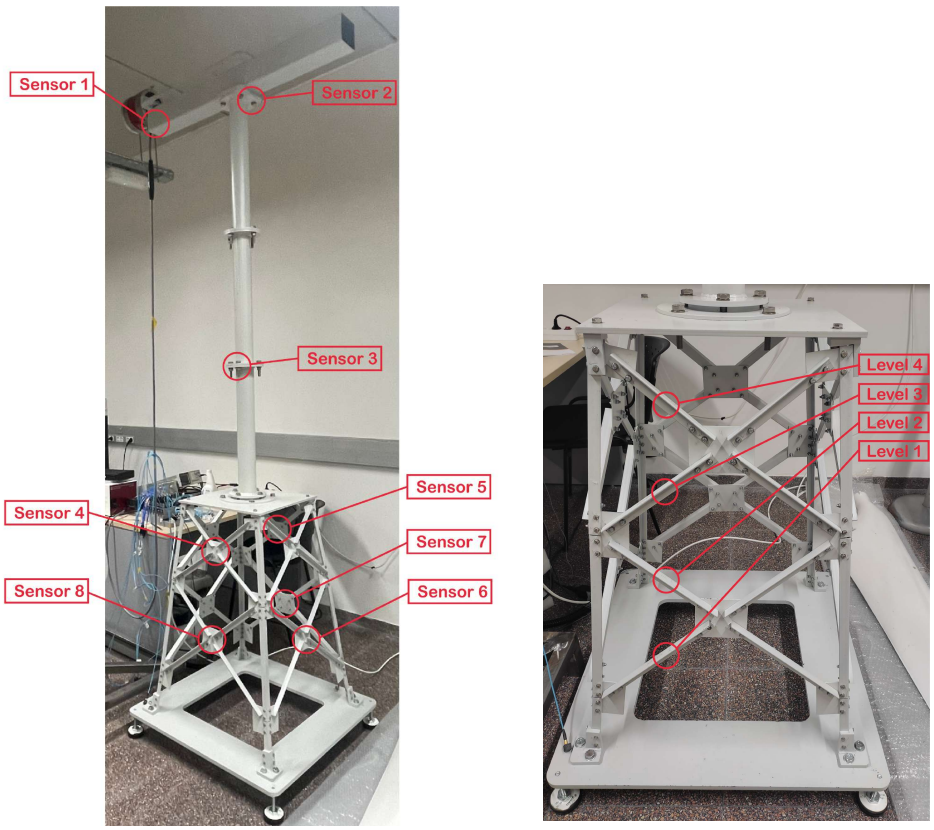

Figure 1: Location of the sensors (accelerometers) within the structure (left). The distinct levels of the jacket support (right).

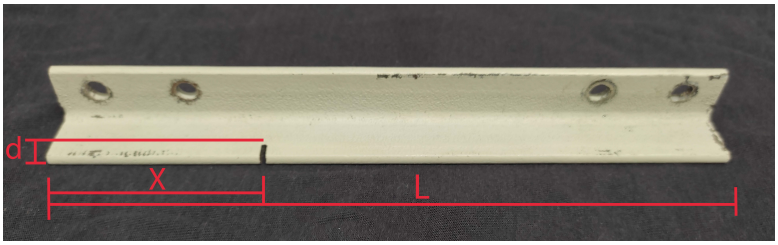

Figure 2: Bar with a 5 mm crack.

3 Data Acquisition

This section delineates the data acquisition methodology employed in the various experiments conducted, simulating various conditions and structural states.

In this work, four experiments are carried out, of which two are carried out on a completely intact (healthy) structure, while one focuses on the Level 1 crack case and the other on the Level 4 crack case. All the cases under a white noise amplitude of 3.

Each experiment spans a duration of 60 seconds, with a sampling frequency set at 1651.6 [Hz], thereby yielding 1651.6 [Hz]×60[s] = 99096 measurements for each experiment. Given the use of 8 triaxial accelerometers, the total number of signals received for each sample measurement amounts to 8×3=24 signals.

The data corresponding to the k-th experiment is encapsulated in a matrix $\mathbf{S}^{(k)}$ with coeffi-

cients $s_{n,m}^{(k)}$ $(n = 1, \ldots, N,\ m = 1, \ldots, M)$ as shown below:

$$S^{(k)} = \begin{bmatrix} s_{1,1}^{(k)} & s_{1,2}^{(k)} & \ldots & s_{1,M}^{(k)} \\ s_{2,1}^{(k)} & s_{2,2}^{(k)} & \ldots & s_{2,M}^{(k)} \\ \vdots & \vdots & \ddots & \vdots \\ s_{N,1}^{(k)} & s_{N,2}^{(k)} & \ldots & s_{N,M}^{(k)} \end{bmatrix}, \tag{1}$$

considering $k \in [1, K]$, where K is 4 in our study. The two subindices in the matrix coefficients correspond to the sample measurement (row) and the vibration signal from the axis of an accelerometer (column), respectively. More precisely,

- $n = 1, \ldots, N$ denotes the time stamps at which the different sample measurements are taken, with N representing the total number of time stamps per experiment, which is equal to 99096;
- $m = 1, \ldots, M$ represents the vibration signals, with M denoting the total number of signals, which in our experiments is equal to 24.

Consequently, each experiment matrix has dimension $S^{(k)} \in \mathbb{M}_{99096\times 24}(\mathbb{R})$. Note that to simplify the notation, the nomenclature for each axis of an accelerometer is not included. For each accelerometer, the axes are always ordered as 1, 2, and 3, from left to right, in the columns of the matrix $S^{(k)}$.

4 Damage Detection Methodology

In this section, the methodology employed for damage detection using the acquired data is introduced. The primary objective is to develop an effective approach to differentiate between healthy and damaged states of structural components. To achieve this, a new data matrix is created that combines a fixed duration of measurements from a healthy structure with a shorter segment of measurements from a damaged structure. This composite matrix enables to discern structural damage based on specific data patterns.

4.1 Constructing the Composite Matrix

Initially, a matrix containing data exclusively from one healthy experiment (called baseline) from the set of two healthy experiments is formed. Let B denote such a baseline matrix:

$$B = \begin{bmatrix} s_{1,1}^{(1)} & s_{1,2}^{(1)} & \ldots & s_{1,M}^{(1)} \\ s_{2,1}^{(1)} & s_{2,2}^{(1)} & \ldots & s_{2,M}^{(1)} \\ \vdots & \vdots & \ddots & \vdots \\ s_{N,1}^{(1)} & s_{N,2}^{(1)} & \ldots & s_{N,M}^{(1)} \end{bmatrix} = \begin{bmatrix} b_{1,1} & b_{1,2} & \ldots & b_{1,M} \\ b_{2,1} & b_{2,2} & \ldots & b_{2,M} \\ \vdots & \vdots & \ddots & \vdots \\ b_{N,1} & b_{N,2} & \ldots & b_{N,M} \end{bmatrix}, \tag{2}$$

where $b_{n,m}$ represents the n-th row and m-th column element of the 60 seconds matrix of known healthy data (baseline), which remains constant for all new composite matrices.

Afterward, test data (5 seconds) coming from each of the remaining 3 experiments with data to be diagnosed (in this case k goes from 2 to 4) are processed. Let T^l denote the test data matrix, which is defined as:

$$T^l = \begin{bmatrix} s^{(k)}_{F,1} & s^{(k)}_{F,2} & \cdots & s^{(k)}_{F,M} \\ s^{(k)}_{F+1,1} & s^{(k)}_{F+1,2} & \cdots & s^{(k)}_{F+1,M} \\ \vdots & \vdots & \ddots & \vdots \\ s^{(k)}_{F+8257,1} & s^{(k)}_{F+8257,2} & \cdots & s^{(k)}_{F+8257,M} \end{bmatrix} = \begin{bmatrix} t^{(l)}_{1,1} & t^{(l)}_{1,2} & \cdots & t^{(l)}_{1,M} \\ t^{(l)}_{2,1} & t^{(l)}_{2,2} & \cdots & t^{(l)}_{2,M} \\ \vdots & \vdots & \ddots & \vdots \\ t^{(l)}_{8258,1} & t^{(l)}_{8258,2} & \cdots & t^{(l)}_{8258,M} \end{bmatrix}, \tag{3}$$

where each T^l matrices represent segments corresponding to a non-overlapping 5-second interval of data extracted from matrix S^k. For example, setting $F = 1$ corresponds to the first 5 seconds of data, $F = 8259$ represents the subsequent 5 seconds, and this pattern continues, causing F to increase by 8258 for the next 5 second segment, and so on. On the other hand, the superscript l represents the number of new matrices formed from the data to be diagnosed, and ranges from 1 to 12 for each experiment k.

Finally, the composite matrices $Y^{(l)}$ are constructed combining the matrix B with one matrix T^l as follows:

$$Y^{(l)} = \begin{bmatrix} b_{1,1} & b_{1,2} & \cdots & b_{1,M} \\ b_{2,1} & b_{2,2} & \cdots & b_{2,M} \\ \vdots & \vdots & \ddots & \vdots \\ b_{N,1} & b_{N,2} & \cdots & b_{N,M} \\ & & & \\ t^{(l)}_{1,1} & t^{(l)}_{1,2} & \cdots & t^{(l)}_{1,M} \\ t^{(l)}_{2,1} & t^{(l)}_{2,2} & \cdots & t^{(l)}_{2,M} \\ \vdots & \vdots & \ddots & \vdots \\ t^{(l)}_{8258,1} & t^{(l)}_{8258,2} & \cdots & t^{(l)}_{8258,M} \end{bmatrix} = \begin{bmatrix} y^{(l)}_{1,1} & y^{(l)}_{1,2} & \cdots & y^{(l)}_{1,M} \\ y^{(l)}_{2,1} & y^{(l)}_{2,2} & \cdots & y^{(l)}_{2,M} \\ \vdots & \vdots & \ddots & \vdots \\ y^{(l)}_{J,1} & y^{(l)}_{J,2} & \cdots & y^{(l)}_{J,M} \end{bmatrix}, \tag{4}$$

where $J = 107354$.

This matrix serves as the foundation for the subsequent analysis. Attention is now directed toward the application of the DDC technique, a powerful approach that utilizes the composite matrix for the accurate classification of unknown structural states. In the following section, details of the DDC technique and its implementation are explored, which sheds light on its effectiveness in distinguishing structural deviations within the experimental data.

4.2 Detect Deviation Cells

For many years, the focus in statistics was on developing robust estimation methods that are less sensitive to entire outlying rows in the data matrix and capable of detecting them (see e.g. [16] and [17]). However, the paradigm of entire outlying rows does not correspond to what often occurs in many applications [18]. For instance, it may happen that most of the data cells in a row are regular, and only a few are anomalous. In the case of WTs application, a measurement of a damaged structure may be considered an outlier due to anomalous accelerometer signals coming from only a few sensors, rather than all of them. Methods designed for detecting row-wise outliers cannot identify the specific cells responsible for a row to be considered an outlier, and are also unsuitable when the data matrix contains more than 50% of contaminated rows. Therefore, in most cases, it is more realistic to assume a cell-wise paradigm, where outliers can be present in individual cells of the data matrix, and employ a cell-wise technique to analyze

the data. The DDC method is a cell-wise outlier filter capable of detecting cell-wise outliers in a data matrix. Moreover, DDC is an unsupervised technique that does not require prior labeling of the structural state for each sample measurement. This characteristic aligns well with real-life problems of SHM of WTs where information about the initial state of the WT to be evaluated is lacking. Another advantage of DDC is its suitability for high-dimensional datasets, as is the case in this study. It also provides robust estimates of the 'true' values of the outlying cells and missing cells by exploiting correlations between variables. Unlike row-wise methods, DDC does not easily break down, even when the data matrix contains more than 50% of contaminated rows. In this work, DDC is utilized to detect WTs with potential damage (crack at level 1 or level 4 of the structure) and the time at which the potential damage occurred. DDC also allows to filtering the sensors (i.e. the location of the structure) that alert to the presence of abnormality. To achieve this, the DDC filter is applied to each of the sample matrices $Y^{(l)} \in \mathbb{M}_{107354\times 24}(\mathbb{R})$. Therefore, the goal is to classify the structural state from the 5-second accelerometer measurements. Note that DDC, as an unsupervised technique, does not need to know the state label of each observation for this task.

DDC assumes that every variable is approximately normally distributed for its regular values. Let $Y = Y^{(l)} = \{y_{j,m}^{(l)}\}$ denote the data matrix of size $J \times M$, that is, with J sample measurements and M signals from the sensors. Note that the superscript l is removed here for ease of notation. The DDC algorithm starts by robustly standardizing the data matrix Y to Z by using a robust univariate estimator of location and a robust univariate estimator of scale (e.g. M-estimators [16]). Let $\hat{\mu}_m$ and $\hat{\sigma}_m$ denote the robust location and the robust scale estimate, respectively, for the variable m. Then, the standardization is done by:

$$z_{j,m} = \frac{y_{j,m} - \hat{\mu}_m}{\hat{\sigma}_m}. \tag{5}$$

Next, DDC applies an initial outlier filtering step for each variable by using a cutoff value c which is defined as:

$$c = \sqrt{\chi^2_{1,q}},$$

where $\chi^2_{1,q}$ is the $q-$th quantile of the chi-squared distribution with one degree of freedom. The default value of q is set to 99% so that ideally only 1% of the entries of a variable are flagged. Then, a new matrix U is created with the following entries:

$$u_{j,m} = \begin{cases} z_{j,m}, & \text{if } |z_{j,m}| \leq c, \\ \text{NA(missing)}, & \text{otherwise.} \end{cases} \tag{6}$$

DDC then uses a robust correlation estimator to identify correlated variables to each target variable m. Variables with absolute robust correlation larger than or equal to 0.5 are used to estimate cells of the target variable that were set to missing (initially flagged cells). Let H_m be the set of all such variables h that are correlated to the variable m, including m itself. Denote by $b_{m,h}$ the slope of a robust regression line without intercept that predicts the variable m using variable h only. The estimated values $\tilde{z}_{j,m}$, $j = 1, \ldots, J$, are then calculated as

$$\tilde{z}_{j,m} = G\left(\{b_{m,h}u_{j,h};\ h \text{ in } H_m\}\right),$$

where G is a combination rule applied to cells $u_{j,h}$ that were not flagged in the initial filtering step (see equation 6). If all cell values in a row $(u_{j,1}, \ldots, u_{j,M})^t$ were initially flagged, then the

combination rule is defined to give a value of 0. Since predictions $\tilde{z}_{j,m}$ tend to shrink the scale of the entries, a deshrinkage step is applied. Let $\hat{z}_{j,m}$ denote the new estimates after deshrinkage. Finally, potential cell-wise outliers are flagged by using standardized cell residuals:

$$r_{j,m} = \frac{z_{j,m} - \hat{z}_{j,m}}{\hat{\sigma}_m \left(z_{j,m} - \hat{z}_{j,m}\right)},$$

where $\hat{\sigma}_m \left(z_{j,m} - \hat{z}_{j,m}\right)$ is a robust univariate scale estimate applied to the differences $(z_{j,m} - \hat{z}_{j,m})$, $j = 1, \ldots, J$. For each variable m, cells with $|r_{j,m}| > c$ are flagged as anomalous. DDC forms an imputed data matrix Z_{imp} by replacing these deviating cells and also the missing values by their estimates $\hat{z}_{j,m}$ while keeping the rest of the cells as in Z. By undoing the standardization step in 5, DDC eventually obtains the imputed data matrix Y_{imp} in the original units. Note that the DDC algorithm also allows to flag an entire row if it contains too many outliers. For a more detailed explanation of the DDC algorithm, we refer the reader to [19] and [20].

5 Results

This section provides and examines the results of the suggested crack damage detection approach in the WT jacket structure. Performance is obtained by calculating the sensitivity and specificity measures. Sensibility is defined here as the percentage of correctly predicted damaged states by DDC among the true damaged states, while specificity indicates the percentage of correctly predicted healthy states by DDC among the true healthy states. The results for the evaluation of structures with cracks at level 1 and level 4 are presented in Table 1. The results show that DDC is highly effective in detecting these states in various time intervals, with a mean specificity of roughly 98% and a mean sensitivity of roughly 99.5% for both crack levels.

	Amplitude 3 - Level 1		**Amplitude 3 - Level 4**	
Interval	**Specificity**	**Sensitivity**	**Specificity**	**Sensitivity**
$[0, 5)$	97.95%	99.30%	97.95%	99.31%
$[5, 10)$	98.00%	99.59%	98.05%	99.61%
$[10, 15)$	97.9%	99.52%	97.94%	99.50%
$[15, 20)$	98.12%	99.59%	98.11%	99.58%
$[20, 25)$	97.99%	99.41%	98.06%	99.38%
$[25, 30)$	97.94%	99.22%	97.93%	99.22%
$[30, 35)$	98.13%	99.61%	98.15%	99.60%
$[35, 40)$	98.07%	99.66%	97.98%	99.67%
$[40, 45)$	98.07%	99.60%	98.07%	99.54%
$[45, 50)$	97.96%	99.46%	98.00%	99.43%
$[50, 55)$	97.84%	99.65%	97.92%	99.64%
$[55, 60]$	97.91%	99.69%	97.86%	99.69%
Mean	97.99%	99.52%	98.00%	99.51%

Table 1: Specificity and sensitivity for the crack structural state level 1 and level 4.

On the other hand, Table 2 shows the specificity for the measurements of the healthy test structure. The results show that DDC identifies when a jacket structure is healthy at various time intervals, with a mean specificity of 99.04%.

Healthy structure

Interval	Specificity
[0,5)	99.08%
[5,10)	99.02%
[10,15)	99.02%
[15,20)	99.02%
[20,25)	99.03%
[25,30)	99.02%
[30,35)	99.02%
[35,40)	99.08%
[40,45)	99.09%
[45,50)	99.02%
[50,55)	99.02%
[55,60]	99.02%
Mean	99.04%

Table 2: Specificity for the healthy structural state.

DDC also identified sensors (cells) responsible for predicting damage to a structure at a specific time (observation). The results are displayed in a plot known as a 'cell map'. The cell map is a graphical representation of the data matrix, with cells colored differently according to whether DDC flagged them as anomalous or not. Figure 3 shows the cell maps for all damage state experiments conducted in this study. The yellow cells represent sensors that provide regular measurements for the corresponding sensor and time. Cells in red correspond to sensors that provide potentially anomalous measurements because they are much higher than expected, whereas cells in blue correspond to sensors with potentially anomalous measurements because they are much lower than expected. To be able to show the results of DDC in the entire matrix, Nblocks of 3976 observations are created, and, as a consequence, the color of each cell represents the 'average color' within the block (as can be seen in Figure 3). Becomes clear that sensors 4 (axis 12) and 7 (axes 19, 20, 21) play a significant role in alerting potential structural damage.

The good performance of DDC with healthy states is evident in Figure 4, where almost all cells are colored yellow, indicating that no sensor indicates any type of anomaly.

6 Conclusion

In this study, a novel data-driven approach is proposed for early damage detection in WTs called "Detect Deviating Cells". This approach leverages triaxial accelerometer data collected from an experimental WT. The results obtained show that DDC is highly effective in predicting a damaged structure (mean sensitivity of roughly 99.50% for both types of damage) and in detecting a healthy structure (mean specificity of 99.04% when all measurements are healthy) using vibration data collected in a short period of time. DDC was also able to identify sensors 4 and 7 as the most sensible to provide an alert of potential damage to the structure.

The promising potential of DDC for damage detection in WTs is demonstrated by our experimental results. Importantly, DDC is an unsupervised technique that does not require

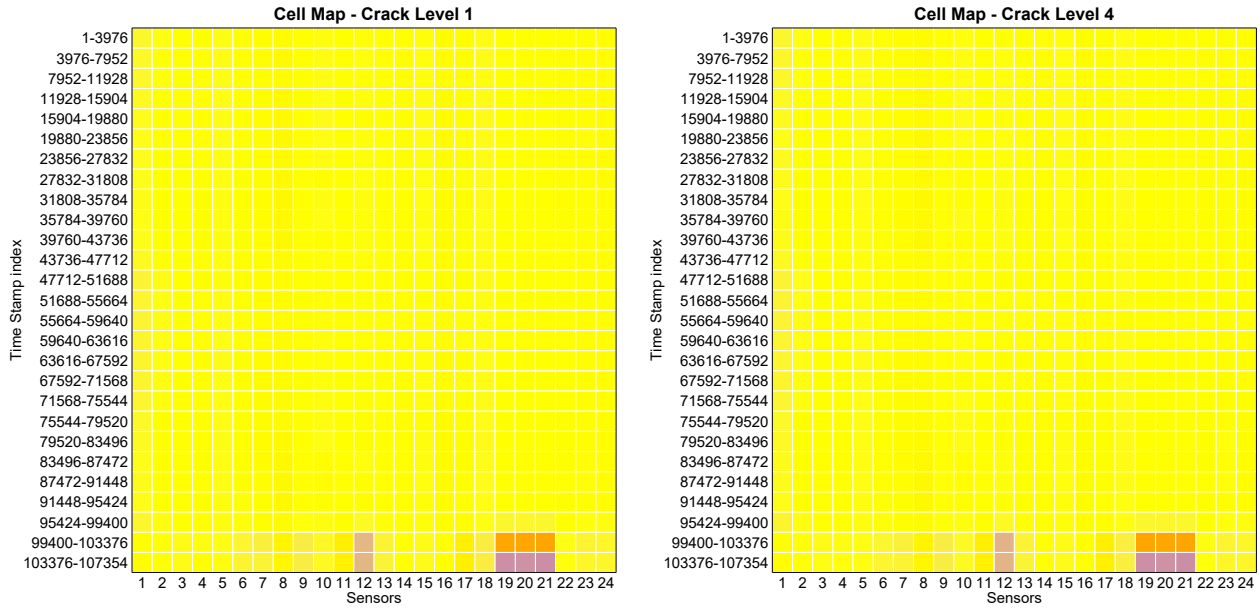

Figure 3: Cell map when predicting the structural state on crack Level 1 (left) and crack level 4 (right) with a value of 3 for the shaker white noise amplitude.

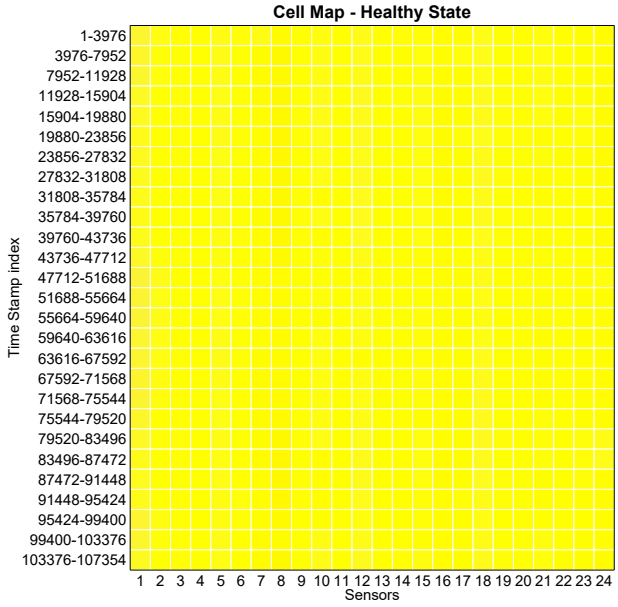

Figure 4: Cell map when predicting the structural state on a healthy structure with a value of 3 for the shaker white noise amplitude.

prior labeling of the WT health status. This characteristic makes DDC suitable for SHM applications where the initial status of wind turbines is unknown and the majority of data may be derived from healthy turbines. Furthermore, DDC can be applied to recently acquired data, allowing timely detection of damages without the need for costly and time-consuming on-site inspections. This capability facilitates prompt repair actions and contributes to an effective, fast, and cost-efficient alternative for SHM. The presented approach can be utilized by WT

operators to mitigate risks, optimize maintenance plans, and ensure the sustained reliability of wind energy systems. In future studies, the potential of DDC to detect damage in offshore wind turbines using experimental data will continue to be explored, taking into consideration additional data as well as other types of damage in the structure and varying shaker white noise amplitudes.

ACKNOWLEDGMENTS

This work is partially funded by the Spanish Agencia Estatal de Investigación (AEI) - Ministerio de Economía, Industria y Competitividad (MINECO), and the Fondo Europeo de Desarrollo Regional (FEDER) through the research projects PID2021-122132OB-C21 and TED2021-129512B-I00; and by the Generalitat de Catalunya through the research project 2021-SGR-01044.

REFERENCES

[1] I. Galparsoro, I. Menchaca, J. M. Garmendia, Á. Borja, A. D. Maldonado, G. Iglesias, and B. Juan, "Reviewing the ecological impacts of offshore wind farms," *npj Ocean Sustainability*, vol. 1, no. 1, p. 1, 2022.

[2] A. G. Olabi, K. Obaideen, M. A. Abdelkareem, M. N. AlMallahi, N. Shehata, A. H. Alami, A. Mdallal, A. A. M. Hassan, and E. T. Sayed, "Wind energy contribution to the sustainable development goals: Case study on london array," *Sustainability*, vol. 15, no. 5, p. 4641, 2023.

[3] A. Q. Al-Shetwi, "Sustainable development of renewable energy integrated power sector: Trends, environmental impacts, and recent challenges," *Science of The Total Environment*, vol. 822, p. 153645, 2022.

[4] V. Magar, A. Peña, A. N. Hahmann, D. A. Pacheco-Rojas, L. S. García-Hernández, and M. S. Gross, "Wind energy and the energy transition: Challenges and opportunities for mexico," *Sustainability*, vol. 15, no. 6, p. 5496, 2023.

[5] W. Strielkowski, L. Civín, E. Tarkhanova, M. Tvaronavičienė, and Y. Petrenko, "Renewable energy in the sustainable development of electrical power sector: A review," *Energies*, vol. 14, no. 24, p. 8240, 2021.

[6] S. Watson, A. Moro, V. Reis, C. Baniotopoulos, S. Barth, G. Bartoli, F. Bauer, E. Boelman, D. Bosse, A. Cherubini, A. Croce, L. Fagiano, M. Fontana, A. Gambier, K. Gkoumas, C. Golightly, M. I. Latour, P. Jamieson, J. Kaldellis, A. Macdonald, J. Murphy, M. Muskulus, F. Petrini, L. Pigolotti, F. Rasmussen, P. Schild, R. Schmehl, N. Stavridou, J. Tande, N. Taylor, T. Telsnig, and R. Wiser, "Future emerging technologies in the wind power sector: A european perspective," *Renewable and Sustainable Energy Reviews*, vol. 113, p. 109270, 2019.

[7] Y. Yang, Y. Zhang, and X. Tan, "Review on vibration-based structural health monitoring techniques and technical codes," *Symmetry*, vol. 13, no. 11, p. 1998, 2021.

[8] A. Silva-Campillo, F. Pérez-Arribas, and J. C. Suárez-Bermejo, "Health-monitoring systems for marine structures: A review," *Sensors*, vol. 23, no. 4, p. 2099, 2023.

[9] J. X. Leon-Medina, M. Anaya, N. Parés, D. A. Tibaduiza, and F. Pozo, "Structural damage classification in a jacket-type wind-turbine foundation using principal component analysis and extreme gradient boosting," *Sensors*, vol. 21, no. 8, p. 2748, 2021.

[10] J. Leng, P. Gardoni, M. Wang, Z. Li, G. Królczyk, S. Feng, A. Incecik, and W. Li, "Condition-based structural health monitoring of offshore wind jacket structures: Opportunities, challenges, and perspectives," *Structural Health Monitoring*, vol. 0, no. 0, 2023.

[11] B. Kim, C. Min, H. Kim, S. Cho, J. Oh, S.-H. Ha, and J.-h. Yi, "Structural health monitoring with sensor data and cosine similarity for multi-damages," *Sensors*, vol. 19, no. 14, p. 3047, 2019.

[12] H. Ye, C. Jiang, F. Zu, and S. Li, "Design of a structural health monitoring system and performance evaluation for a jacket offshore platform in east china sea," *Applied Sciences*, vol. 12, no. 23, p. 12021, 2022.

[13] F. Zonzini, F. Romano, A. Carbone, M. Zauli, and L. De Marchi, "Enhancing vibration-based structural health monitoring via edge computing: A tiny machine learning perspective," in *Quantitative Nondestructive Evaluation*, vol. 85529. American Society of Mechanical Engineers, 2021, p. V001T07A004.

[14] M. d. C. Feijóo, Y. Zambrano, Y. Vidal, and C. Tutivén, "Unsupervised damage detection for offshore jacket wind turbine foundations based on an autoencoder neural network," *Sensors*, vol. 21, no. 10, p. 3333, 2021.

[15] B. Puruncajas, Y. Vidal, and C. Tutivén, "Vibration-response-only structural health monitoring for offshore wind turbine jacket foundations via convolutional neural networks," *Sensors*, vol. 20, no. 12, p. 3429, 2020.

[16] R. A. Maronna, R. D. Martin, V. J. Yohai, and M. Salibián-Barrera, *Robust statistics: theory and methods (with R)*. John Wiley & Sons, 2019.

[17] H. Cevallos-Valdiviezo and S. Van Aelst, "Fast computation of robust subspace estimators," *Computational Statistics & Data Analysis*, vol. 134, pp. 171–185, 2019.

[18] H. Cevallos-Valdiviezo, A. Rodríguez-Cristiansen, and P. Valdiviezo-Valenzuela, "Robust estimation of principal components: a literature review," in *20th LACCEI International Multi-Conference for Engineering, Education, and Technology*, 2022.

[19] P. J. Rousseeuw and W. V. D. Bossche, "Detecting deviating data cells," *Technometrics*, vol. 60, no. 2, pp. 135–145, 2018.

[20] H. Cevallos-Valdiviezo, M. Valero-Carrera, A. Rodríguez-Cristiansen, P. Valdiviezo-Valenzuela, E. García-Ochoa, and D. Arévalo-Avecillas, "Non-technical loss detection based on electricity consumption data: A case study in Ecuador," in *Proceedings of the 11th International Conference on Software and Information Engineering*, 2022, pp. 66–71.